

Controlled Synthesis of Silver Nanowires: Production and Characterization

S.G. NURIYEVA^a, H.A. SHIRINOVA^{a,*},
K.M. HASANOV^b AND F.V. HAJIYEVA^a

^a*Baku State University, Acad. Z. Khalilov street 23, AZ 1148, Baku, Azerbaijan*

^b*Institute of Radiation Problems, B. Vahabzadeh street 9, AZ 1143, Baku, Azerbaijan*

Received: 02.11.2022 & Accepted: 20.02.2023

Doi: [10.12693/APhysPolA.143.279](https://doi.org/10.12693/APhysPolA.143.279)

*e-mail: aliyeva.sevinj.garib@gmail.com

In this study, silver nanowires have been synthesized by the modified polyol method. Atomic force microscopy and optical microscopy were used to study the morphological properties of nanowires. The average diameter and length of obtained silver nanowires were 40–80 nm and 2–6 μm , respectively. Moreover, the investigation showed that the morphology of synthesized nanostructures dramatically depends on the concentration of halides. X-ray diffractometer study of the nanowires confirmed that the growth process occurs through the deposition of Ag^+ ions onto the (111) plane. The ultraviolet-visible spectroscopy analysis demonstrated two localized surface plasmon resonance vibration lines of silver nanowires. The study determined that the blue shift of these vibration lines occurred due to the change in the size of the nanowires and depended on the halide concentration. The photoluminescence spectra of samples demonstrated two emission maximums in blue–green regions related to radiative recombination of Fermi level electrons and *sp*- or *d*-band holes.

topics: silver nanowires, polyol method, localized surface plasmon resonance, blue–green luminescence

1. Introduction

One-dimensional (1D) metal nanostructures have various applications due to their unique electrical, optical, thermal, mechanical, and catalytic properties and thus have been the focus of recent research. Characteristics of the silver nanowires (Ag NWs) depend strongly on their size and morphology. The development of an optimal physical or chemical synthesis method, which allows accurate control of the size and morphology of the nanowires, is vital for their feature formation. Various techniques of synthesis and stabilization of Ag NWs have been reported. One of the effective synthesis methods is the hydrothermal method [1]. Scientists report that Ag NWs produced by the hydrothermal method possess non-linear optical properties and could be applied to filler laser [1]. In addition, it is possible to produce Ag NWs with 100 nm in diameter and a length of 800 μm with the help of the hydrothermal method [2]. Another research group has succeeded in synthesizing silver nanowires with a diameter of \simeq 45–65 nm and a length of more than 200 μm using the same method [3]. The solvothermal method is also a commonly used method for the synthesis of Ag NWs [4]. However, the majority of synthesis methods for these materials imposed several technological requirements, such as the introduction

of the reagents into the system drop by drop [4–7]. In this regard, the polyol method is widely used as one of the simplest methods in the synthesis of Ag NWs [8, 9]. Furthermore, the polyol method is also an effective technique due to its low cost, mild reaction conditions, and suitability for industrial production [10, 11]. Jung et al. [9] introduced a “one-pot” process for the synthesis of Ag NWs with a length of 100 μm and 100 nm in diameter using the polyol method. Recently, there have been produced Ag NWs with a 20 nm diameter and a high aspect ratio of 2000 with the help of the “one-pot” technique [12].

According to the literature review, it can be concluded that the influence of various parameters on the growth mechanism of silver nanowires has been studied well. However, the majority of the suggested techniques are either inapplicable to mass production or the production technique is too complex for a commercial purpose [13].

Herein, Ag NWs also were synthesized by a polyol method. However, unlike the traditional polyol method, in this work, for the first time, all reagents were introduced into the system simultaneously, which made the synthesis method quite simple. In addition, the effective ratio of initial reagents during the synthesis of silver nanowires for large-scale production for industrial purposes was determined.

2. Materials and methods

2.1. Materials

Silver nitrate (AgNO_3 , 98%), sodium chloride (NaCl , 99.9%), potassium bromide (KBr , 99.0%), polyvinylpyrrolidone ($(\text{C}_6\text{H}_9\text{NO})_n$, $\text{MW} \approx 1300000$), ethylene glycol ($(\text{CH}_2\text{OH})_2$, 99.8%), and ethanol ($\text{C}_2\text{H}_6\text{O}$, 99.7%) were purchased from Karma Lab (Izmir, Turkey). All chemicals were of analytical grade.

2.2. Preparation

A modified polyol method with two halides was used to produce Ag NWs with a high aspect ratio [7]. Ethylene glycol (EG) solutions of the 0.01 M NaCl and 0.005 M KBr salts were prepared. Subsequently, 0.6 g polyvinylpyrrolidone (PVP) was solved in 20 ml EG at the 100°C . Finally, 0.6 g AgNO_3 , 0.6 ml NaCl/EG, and 1.6 ml KBr/EG solutions were added to the PVP/EG system and intensively mixed for a minute. The process continued in a silicone oil bath heated to a temperature of 175°C for 13–17 min (Fig. 1). The mixture was diluted with ethanol and centrifuged several times to remove excess reagents until the transparent solution was obtained. No need to add the reagents slowly or drop by drop is the main advantage of the chosen method.

2.3. Characterization

The microstructure of Ag NWs samples was studied on an optical microscope Zeiss Axio Imager.A2m. The ultraviolet-visible (UV-vis) spectrum has been recorded on a spectrophotometer Specord 250 Plus at the 200–700 nm range. The X-ray powder diffraction (XRD) patterns were examined by diffractometer Rigaku MiniFlex 600s using the copper anode ($\text{Cu } K_\alpha$ radiation, 30 kV and 15 mA) at room temperature. The samples were scanned in the range of 2θ angle of 10–80. The

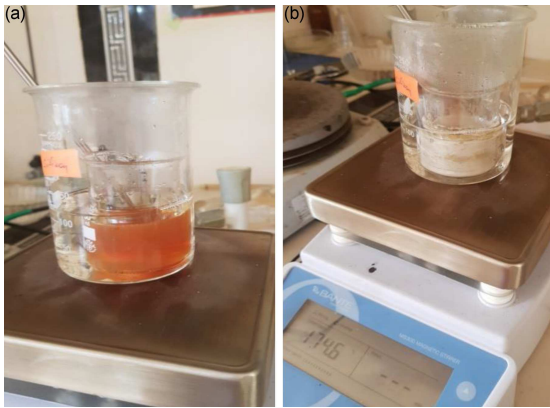


Fig. 1. Synthesis process of Ag NWs.

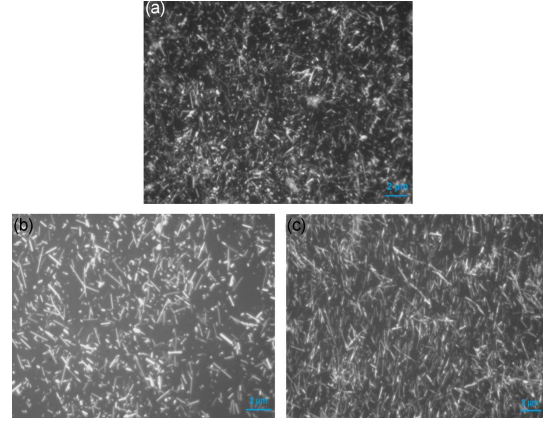


Fig. 2. The images of Ag NWs from an optical microscope: (a) Ag (1:1); (b) Ag (2:1); (c) Ag (1:2).

Marphological data of produced Ag NWs. TABLE I

Sample nomination	Concentration		Morphology of synthesized Ag^0
	NaCl	KBr	
Ag (1:1)	0.01 M	0.01 M	mainly nanoparticles rather than nanowires
Ag (2:1)	0.01 M	0.005 M	$\bar{d} = 80 \text{ nm}$ $\bar{l} = 2\text{--}4 \mu\text{m}$
Ag (1:2)	0.005 M	0.01 M	$\bar{d} = 55 \text{ nm}$ $\bar{l} = 3\text{--}6 \mu\text{m}$

morphology of the Ag NWs was studied by using Integra Prima atomic force microscope (AFM) (NT-MDT). The measurement was performed in the semi-contact mode in the open air. The luminescence properties of Ag NWs were investigated by the Cary Eclipse spectrofluorometer.

3. Result and discussion

Figure 2 demonstrates the image of Ag NWs from an optical microscope. It is clear that the morphology formation of the samples significantly depends on the concentration of Br^- and Cl^- ions. Research shows that the absence of Cl^- ions leads to the formation of only Ag nanoparticles. Similarly, when NaCl is the only control agent (in the absence of Br^- ions), the coarser Ag nanorods and nanoparticles were formulated [14]. The summary of the microscopic investigation of produced nanostructures was collected in Table I.

According to the table, when the weight ratio of the Cl^- and Br^- ions is 1:1, mainly nanoparticles were obtained rather than nanowires (Fig. 2a). A twice reduction of the KBr concentration stimulates Ag to grow as a 1D nanostructure with approximately 80 nm in diameter and 2–4 μm of length (Fig. 2b). In contrast, when the concentration of NaCl is lower than that of KBr, the decreasing diameter and increasing length of the formulated one-dimensional nanostructures are observed (Fig. 2c).

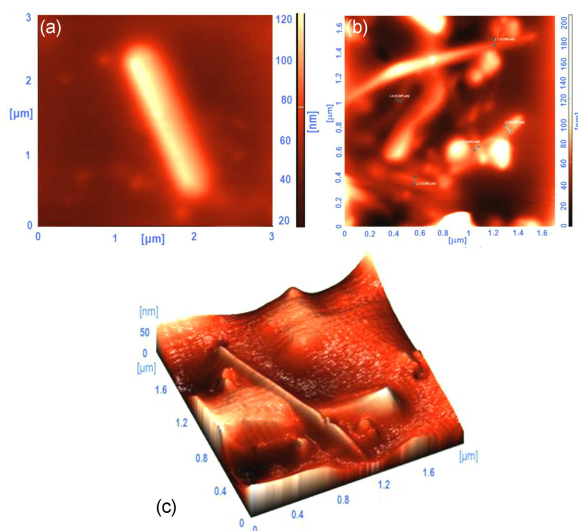


Fig. 3. AFM images of Ag (1:2): (a) 2D image; (b) 3D image.

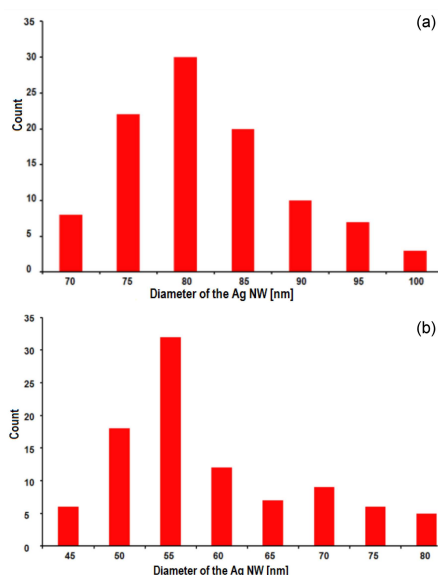


Fig. 4. The diameter distribution of the Ag NW (a) Ag (2:1); (b) Ag (1:2).

Figure 3 shows the 2D and 3D AFM topography of Ag (1:2). This study also proves the formation of the nanowires. In Fig. 4, the diameter distribution histogram of the Ag nanowires is shown.

The crystalline structure of synthesized nanowires was investigated by an X-ray diffractometer (Fig. 5). The characteristic lines at the 38.67° , 44.73° , 64.79° , 77.77° , and 81.89° values of 2θ correspond to (111), (200), (220), (311), and (222) indexes, respectively [14]. Regarding the ICDD database (card number 00-004-0783), this pattern belongs to Ag NWs. According to the XRD pattern of the Ag NWs, it can be concluded that nanowires possess face-centered cubic unit cell structure, and

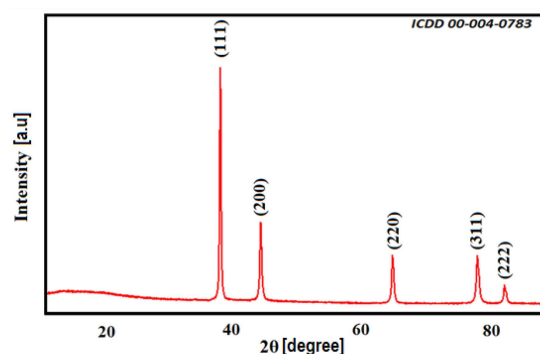


Fig. 5. XRD pattern of Ag NWs.

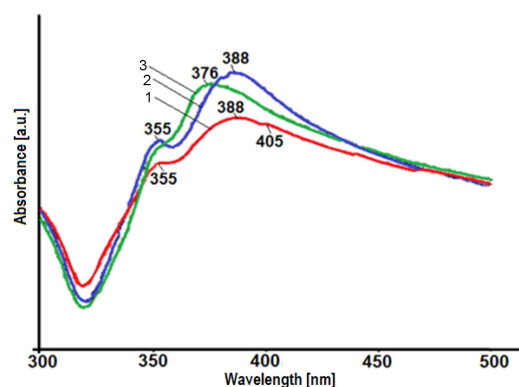


Fig. 6. UV-Vis spectrum of Ag nanostructures: (1) Ag (1:1); (2) Ag (2:1); (3) Ag (1:2).

lattice parameters are $a = b = c = 4.086 \text{ \AA}$ and $\alpha = \beta = \gamma = 90^\circ$, respectively. Uniform nanowires were obtained through the slow release of Ag^+ ions and the fast growth rate of the (111) plane.

Since the growth rate of the (100) plane of Ag NWs is inhibited by the presence of Br^- and Cl^- ions and PVP chains, deposition goes onto the (111) plane [14].

UV-Vis spectra of Ag nanostructures synthesized by different concentration of NaCl and KBr salts is given in Fig. 6. Two characteristic peaks around 355 nm and 388 nm correspond to the localized surface plasmon resonance vibrations of the Ag NWs and are observed for all three samples. The weak peak that appears at about 355 nm is assigned to the quadrupole resonance excitation of Ag NWs [15]. This peak remained stable regardless of the concentration of halides. However, a resonance peak at 388 nm shifted towards lower wavelengths (376 nm) for Ag NWs (1:2) sample (Fig. 6, line 3). This absorption line corresponds to the transverse localized surface plasmon resonance (LSPR) vibration of Ag NWs [15]. The transverse LSPR is sensitive to the size change of the nanowire. The blue shift in the transverse LSPR line is due to the decrease in the diameter of the nanostructures for Ag NWs (1:2) [16–18]. The absorption line at 405 nm is observed only for Ag (1:1) samples and belongs

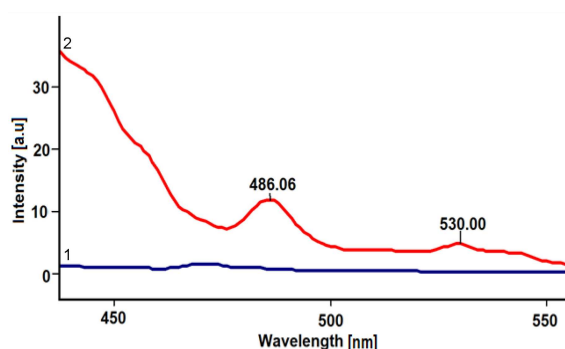


Fig. 7. FL spectrum of Ag NWs: (1) pure ethanol; (2) ethanol+Ag NWs solution.

to surface plasmon vibrations in the silver nanoparticles (Fig. 6, line 1) [19, 20]. The UV-Vis results demonstrate good agreement with microscopic investigation.

The room-temperature fluorescence emission spectra of silver nanostructures were also studied. The excitation wavelength was 414 nm [21]. The photoluminescence (PL) emission of the pure ethanol and the Ag NWs dispersed in ethanol were recorded in the 430–580 nm diapasons (Fig. 7, lines 1 and 2).

Two emission maximums in blue–green regions, namely, 486 nm and 530 nm, were observed in the PL spectrum of silver nanowires. The blue–green emission in the PL spectrum of Ag NWs is due to the radiative recombination of electrons and holes near the Fermi level [21]. It is known that the band structure of the noble metals could be explained in the framework of the free electron gas model. Half-filled $5sp$ band of Ag nanowires is a conduction band and is located above the Fermi level [22]. Fully-filled $4d$ band is a valance band [23]. Photo-excitation leads to the transfer of electrons from the $4d$ band to the $5sp$ band, and holes occur in the $4d$ band. The direct recombination of $4d$ holes and $5sp$ electrons results in visible emission [24].

4. Conclusions

A modified polyol method with two halides, namely, NaCl and KBr, was used to produce Ag NWs. The morphology of Ag nanostructures significantly depended on the ratio of Br^- and Cl^- ions. The experimental investigation showed that at a 1:1 ratio of Cl^- and Br^- ions, mainly nanoparticles were obtained rather than nanowires. A twice reduction of the KBr concentration stimulated Ag to grow as a 1D nanostructure with approximately 80 nm in diameter and 2–4 μm of length. In contrast, when the concentration of NaCl was lower than that of KBr, the formation of Ag nanowires with a diameter of 55 nm and a length of 3–6 μm was observed. X-ray diffractometer study of silver nanowires confirmed that the wires grow through

the deposition of Ag ions onto the (111) plane. In addition, the UV-Vis investigation demonstrated two LSPR vibration lines of Ag NWs. The absorption line at 405 nm was observed only for samples produced at a 1:1 ratio of Cl^- and Br^- ions, which proves the formation of silver nanoparticles besides nanowires. The PL spectra of silver nanowires demonstrated two emission maximums in blue–green regions related to radiative recombination of Fermi level electrons and sp - or d -band holes.

References

- [1] W.J. Liu, M.L. Liu, S. Lin, J.C. Liu, M. Lei, H. Wu, C.Q. Dai, Z.Y. Wei, *Opt. express* **27**, 16440 (2019).
- [2] M. Ćwik, D. Buczyńska, K. Sulowska, E. Roźniecka, S. Mackowski, J. Niedziółka-Jönsson, *Materials* **12**, 721 (2019).
- [3] B. Bari, J. Lee, T. Jang, P. Won, S.H. Ko, K. Alamgir, M. Arshad, L.J. Guo, *J. Mater. Chem. A* **4**, 11365 (2016).
- [4] W.C. Zhang, X.L. Wu, H.T. Chen, Y.J. Gao, J. Zhu, G.S. Huang, P.K. Chu, *Acta Mater.* **56**, 2508 (2008).
- [5] Xiaoli Wu, Zhimin Zhou, Yuehui Wang, Jingze Li, *Coatings* **10**, 865 (2020).
- [6] Yugang Sun, Younan Xia, *Adv. Mater.* **14**, 833 (2002).
- [7] S. Coskun, B. Aksoy, H.E. Unalan, *Cryst. Growth Design* **11**, 4963 (2011).
- [8] Y.E. Shi, L. Li, M. Yang, X. Jiang, Q. Zhao, J. Zhan, *The Analyst* **139**, 2525 (2014).
- [9] J. Jung, H. Lee, I. Ha, H. Cho, K.K. Kim, J. Kwon, P. Won, S. Hong, S.H. Ko, *ACS Appl. Mater. Interfaces* **9**, 44609 (2017).
- [10] S.H. Mirjalili, M.R. Nateghi, F. Kalantari-Fotooh, *J. Text. Inst.* **111**, 139 (2019).
- [11] I.S. Jin, H.D. Lee, S.I. Hong, W. Lee, J.W. Jung, *Polymers* **13**, 586 (2021).
- [12] Y. Li, X. Yuan, H. Yang, Y. Chao, S. Guo, C. Wang, *Materials* **12**, 401 (2019).
- [13] C.A. Charitidis, *Manuf. Rev.* **1**, 19 (2014).
- [14] L. Cao, Q. Huang, J. Cui, H. Lin, W. Li, Z. Lin, P. Zhang, *Nanomaterials* **10**, 1139 (2020).
- [15] C. Wu, X. Zhou, J. Wei, *Nanoscale Res. Lett.* **10**, 354 (2015).
- [16] E.J. Lee, M.H. Chang, Y.S. Kim, J.Y. Kim, *APL Mater.* **1**, 042118 (2013).
- [17] S. Raza, N. Stenger, S. Kadkhodazadeh, S.V. Fischer, N. Kostasheva, A.P. Jauho, A. Burrows, M. Wubs, N.A. Mortensen, *Nanophotonics* **2**, 131 (2013).

- [18] X.M. Wang, L. Chen, E. Sowade, R.D. Rodriguez, E. Sheremet, C.M. Yu, R.R. Baumann, J.J. Chen, *Nanomaterials* **10**, 237 (2020).
- [19] M. Riaz, U. Sharafat, N. Zahid, M. Ismail, J. Park, B. Ahmad, N. Rashid, M. Fahim, M. Imran, A. Tabassum, *ACS Omega* **7**, 14723 (2022).
- [20] M. Ider, K. Abderrafi, A. Eddahbi, S. Ouaskit, A. Kassiba, *J. Clust. Sci.* **28**, 1051 (2017).
- [21] R. Sarkar, P. Kumbhakar, A.M. Mitra, R. Ganeev, *Curr. Appl. Phys.* **10**, 853 (2010).
- [22] M.J. Islam, A. Kumer, *SN Appl. Sci.* **2**, 251 (2020).
- [23] I. Abbati, L. Braicovich, G. Rossi, I. Lindau, U. del Pennino, S. Nannarone, *Phys. Rev. Lett.* **50**, 1799 (1983).
- [24] A. Mooradian, *Phys. Rev. Lett.* **22**, 185 (1968).